NATURAL CONVECTION IN A POROUS SQUARE CAVITY FILLED WITH A TERNARY HYBRID NANOFLUID: A NUMERICAL STUDY

Cornelia Revnic[a], Teodor Groșan[b], Khalil M. Khanafer[c], Ioan Pop[b*]

[a]Faculty of Pharmacy, University of Medicine and Pharmacy,
Cluj Napoca 400012
[b]Department of Mathematics, Faculty of Mathematics and Computer
Science, Babeș-Bolyai University, Cluj-Napoca, Romania
[c]Division of Engineering Technology, College of Innovation and Technology,
University of Michigan-Flint, USA

*Corresponding author (Ioan Pop) (Email: popm.ioan@yahoo.co.uk)

A new theoretical ternary hybrid nanofluid, by suspending three types of nanoparticles with different physical and chemical bonds in a porous square cavity, is proposed in this paper. The ternary hybrid nanofluid is formed by suspending three types of nanoparticles with different physical and chemical bonds into a base fluid. In this study, the nanoparticles Alumina (Al_2O_3), Copper (Cu) and Titania (TiO_2) are suspended into water (H_2O) thus forming the combination. The system of governing partial differential equations, are numerically solved using finite element formulation based on the Galerkin along with ADINA software (Adina v 9.20) method. The average Nusselt number $\overline{Nu}$ is computed for three values of the Rayleigh number: 10, 100 and 1000, with the results of other authors from the open literature. An excellent agreement, and therefore, we are deeply confident that the numerical results obtained are correct and very accurate. We wish to point out that the numerical results of the present paper are completely new and original with very important results for practical applications of the ternary hybrid nanofluid in the modern industry. To our best of knowledge, the results of the present paper were never published by any researcher.

Keywords: *porous cavity; ternary fluids; numerical simulation*

1. Introduction

The interest about porous media has been motivated by the fact that thermally driven flows in porous media have considerable applications in mechanical, chemical and civil engineering.

Applications include food processing and storage, fibrous insulation, thermal insulation of buildings, geophysical systems, electro chemistry, metallurgy, the design of pebble bed nuclear reactors, underground disposal of nuclear or non-nuclear waste, solar power collectors, nuclear reactors, geothermal applications, etc. (Nield and Bejan [1]).

According to Choi [2], the major properties of the nanofluids are homogeneity, long-term stability, minimum clogging in a small number of passageways and increased the heat transmission of the base fluid. A very good collection of published papers on nanofluid can be found in the book by Merkin et al. [3]. It was stated in a review paper by Huminic and Huminic [4] that, during the recent several years, a novel class of working fluids which consists from two solid materials dispersed in a conventional fluid was developed and intensely studied. These fluids are called hybrid nanofluids. The hybrid nanofluids leads to an increased thermal conductivity and finally to a heat transfer enhancement in heat exchangers. The use of nanoparticles in the fluid is a result of the need to increase thermal conductivity and improve heat transfer. In recent times, there has been a considerable amount of interest in developing hybrid nanofluids more extensively. Researchers have composited the, three distinct kinds of nanoparticles into the base fluid, which has resulted in a unique nanofluid classified as a ternary hybrid nanofluid. These ternary hybrid nanofluids have qualities that are much superior to those of binary and hybrid nanofluids in terms of their ability to transport heat. Nanofluids, along with their improved versions (ternary nanofluids), have a highly rich thermal mechanism.

2. Basic equations

Consider the free convection in a two-dimensional porous square cavity filled with a ternary hybrid nanofluid. A schematic geometry of the problem under investigation is shown in Fig. 1, where (x, y) are the Cartesian coordinates and L is the height of the cavity.

With these assumptions, the continuity, Darcy and energy equations are (see Nield and Bejan [1]; Manjumatha et al. [5])

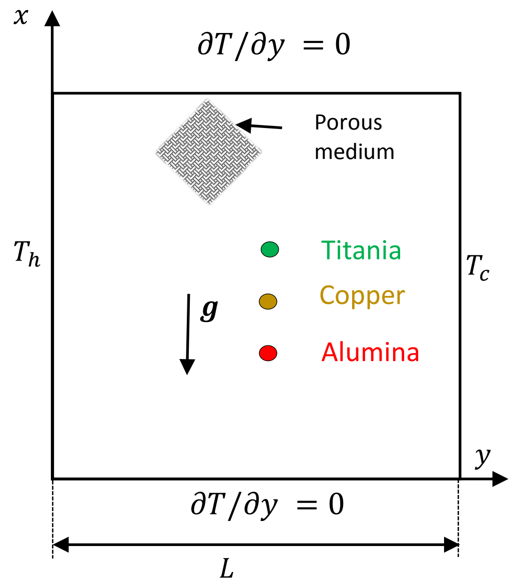

Fig. 1. Physical model and Coordinate system

$$\frac{\partial u}{\partial \bar{x}} + \frac{\partial v}{\partial \bar{y}} = 0 \tag{1}$$

$$\frac{u_t\, \mu_{thnf}}{K} = -\frac{1}{\rho_{thnf}}\frac{\partial p}{\partial x} - \rho_{tf}\, g, \frac{v_t \mu_{thnf}}{K} = -\frac{1}{\rho_{thnf}}\frac{\partial p}{\partial y} \tag{2}$$

where K is the permeability of the porous medium, g is gravitation velocity and ρ_{tf} is the density of the fluid, which is given by the approximation of Bossiness

$$\rho_{tf} = \rho_{thnf}\left[1 - \beta_{thnf}\,(T - T_c)\right] \tag{3}$$

Eliminating the pressure p by cross differentiation between Eqs. (2) and (3), we get

$$\frac{\partial u}{\partial y} - \frac{\partial v}{\partial x} = gK\beta_{thnf}\frac{\rho_{hnf}}{\mu_{hnf}}\frac{\partial T}{\partial y} \tag{4}$$

$$u\,\frac{\partial T}{\partial x} + v\,\frac{\partial T}{\partial y} = \frac{k_{thnf}}{(\rho\, C_p)_{thnf}}\left(\frac{\partial^2 T}{\partial x^2} + \frac{\partial^2 T}{\partial y^2}\right) \tag{5}$$

subject to the boundary condition

$$\begin{aligned} &u(0,y) = v(0,y) = 0 && T(0,y) = T_h \\ &u(L,y) = v(L,y) = 0 && T(L,y) = T_c \\ &u(x,0) = v(x,0) = 0 && \frac{\partial T}{\partial y}(x,0) = 0 \\ &u(x,L) = v(x,L) = 0 && \frac{\partial T}{\partial \bar{y}}(x,L) = 0 \end{aligned} \tag{6}$$

Here (u, v) are the velocity component along $(x, y) -$ axes, T represents the temperature of the ternary hybrid nanofluid, g is the gravitation velocity, K is the permeability of the porous medium. Additionally, for the ternary hybrid nanofluid's the thermal characteristics are: dynamic viscosity, density, heat capacity, thermal conductivity and thermal expansion coefficient, which are represented μ_{thnf}, ρ_{tnhf}, $(\rho\ C_p)_{thnf}$, k_{thnf} and β_{thnf} are given in Table 1.

Table 1. Thermophysical properties with respect to ternary hybrid nanofluid (see Manjunatha et al. [5])

Properties	**Ternary hybrid nanofluid**
Dynamic viscosity	$= \frac{\mu_{nf}}{(1-\varphi_1)^{2.5}(1-\varphi_2)^{2.5}(1-\varphi_3)^{2.5}}$
Density	$\rho_{thnf} = (1-\phi_3)\{(1-\phi_2)[(1-\phi_1)\rho_f + \phi_1\rho_{n1}] + \phi_2\rho_{n2}\} + \phi_3\rho_{n3}$
Thermal capacity	$(\rho C_p)h_{thnf} = (1-\phi_3)\{(1-\phi_2)[(1-\phi_1)(\rho C_p)_f + \phi_1(\rho C_p)_{n1}] + \phi_2(\rho C_p)_{n2}\} + \phi_3(\rho C_p)_{n3}$
Thermal conductivity	$k_{thnf} = \frac{k_3 + 2k_{hnf} - 2\phi_3(k_{hnf} - k_1)}{k_3 + 2k_{hnf} + \phi_3(k_{hnf} - k_1)} \times k_{hnf}$ where $k_{nf} = \frac{k_{n1} + 2k_f - 2\phi_1(k_f - k_{n1})}{k_{n1} + 2k_f + \phi_1(k_f - k_{n1})} \times (k_f)$ $k_{hnf} = \frac{k_{n2} + 2k_{nf} - 2\phi_2(k_{nf} - k_{n2})}{k_{n2} + 2k_{nf} + \phi_2(k_{nf} - k_{n2})} \times (k_{nf})$
Thermal expansion coefficient	$(\rho\ \beta)_{thnf} = (1-\phi_3)\{(1-\phi_2)[(1-\phi_1)(\rho\beta)_f + \phi_1(\rho\beta)_{n1} + \phi_2(\rho\beta)_{n2}$ $\phi_3(\rho\beta)_{n3}$

Table 2. Thermo-physical properties (see Mahmood et al. [6] and [7]).

Physical properties	H_2O $(Water)$	Al_2O_3 (ϕ_1) $(Alumina)$	Cu (ϕ_2) $(Copper)$	TiO_2 (ϕ_3) $(Titanium)$
$\varrho\ (kg/m^3)$	997.1	3970	8933	4250
$C_p(J/kgK)$	4179	765	385	686.2
$k(W/mK)$	0.613	40	400	8.9538

3. Solution

Introducing the dimensionless stream function ψ as

$$u = \left(\frac{\alpha_f}{L}\right)\frac{\partial\psi}{\partial y} \; and \;\; v = -\left(\frac{\alpha_f}{L}\right)\frac{\partial\psi}{\partial x} \tag{7}$$

Equations (4) and (5) along with the boundary conditions (6), reduce to the following boundary problems

$$\frac{\partial^2\psi}{\partial\, y^2} = Ra\varphi_1(\phi_1,\phi_2,\phi_3)\varphi_2(\phi_1,\phi_2,\phi_3)\frac{\partial\theta}{\partial\, y} \tag{8}$$

$$\frac{\partial\psi}{\partial\, y}\frac{\partial\,\theta}{\partial\, x} - \frac{\partial\,\psi}{\partial\, x}\frac{\partial\,\theta}{\partial\, y} = \varphi_3(\phi_1,\phi_2,\phi_3)\left(\frac{\partial^2\theta}{\partial\, x^2} + \frac{\partial^2\theta}{\partial\, y^2}\right) \tag{9}$$

The corresponding boundary conditions of these equations are given by

$$\begin{aligned} &\psi(0,y) = 0 && \theta(0,y) = 1.0 \\ &\psi(1,y) = 0 && \theta(1,y) = 0.0 \\ &\psi(x,0) = 0 && \frac{\partial\,\theta}{\partial\, y}(x,0) = 0 \\ &\psi(x,1) = 0 && \frac{\partial\theta}{\partial y}(x,1) = 0 \end{aligned} \tag{10}$$

where $Ra = gK\beta_f\Delta TL/\alpha_f\nu_f$ is the Rayleigh number, and $\varphi_1(\phi)$, $\varphi_2(\phi)$, and $\varphi_3(\phi)$ are given by

$$\begin{gathered} \varphi_1(\phi_1,\phi_2,\phi_3) = \beta_{thnf}/\beta_f, \quad \varphi_2(\phi_1,\phi_2,\phi_3) = \frac{\rho_{thnf}/\rho_f}{\mu_{thnf}/\mu_f}, \\ \varphi_3(\phi_1,\phi_2,\phi_3) = \frac{k_{thnf}/k_f}{(\rho C_p)_{tnhf}/(\rho C_p)_f} \end{gathered} \tag{11}$$

The physical quantities of interest are the local Nusselt number Nu_y and average Nusselt number $\overline{Nu}$, which are defined as

$$Nu_y = \frac{L}{\Delta T}\frac{k_{thnf}}{k_f}\left(-\frac{\partial\, T}{\partial\, x}\right)_{y=0}, \quad \overline{Nu} = \frac{1}{L}\int_0^L Nu_y d\, y \tag{12}$$

Using (7) and (12) we obtain

$$Nu_y = \frac{k_{thnf}}{k_f}\left(-\frac{\partial\,\theta}{\partial\, x}\right)_{y=0}, \quad \overline{Nu} = \int_0^1 Nu_y d\, y \tag{13}$$

4. Numerical method

If $\phi_1 = \phi_2 = \phi_3 = 0$ (classical porous medium cavity), Eqs. (8) and (9) reduce to

$$\frac{\partial^2\psi}{\partial x^2}+\frac{\partial^2\psi}{\partial y^2}=Ra\frac{\partial \theta}{\partial y}$$

$$\frac{\partial\psi}{\partial y}\frac{\partial \theta}{\partial x}-\frac{\partial \psi}{\partial x}\frac{\partial \theta}{\partial y}=\frac{\partial^2\theta}{\partial x^2}+\frac{\partial^2\theta}{\partial y^2}$$

$$\begin{aligned}
&\psi(0,y)=0 && \theta(0,y)=1.0\\
&\psi(1,y)=0 && \theta(1,y)=0.0\\
&\psi(x,0)=0 && \frac{\partial \theta}{\partial y}(x,0)=0.0\\
&\psi(x,1)=0 && \frac{\partial\theta}{\partial y}(x,1)=0.0
\end{aligned} \tag{14}$$

The boundary value problem (14) has been numerically solved by using a finite element formulation based on the Galerkin method along with ADINA software (Adina v 9.20). A variable grid-size system was employed to capture the rapid changes in the dependent variables especially in the vicinity of the walls where the major gradients occur inside the boundary layer. As such, a non-uniform mesh of 120×120 nodes were found satisfactory with a convergence criterion of error less than 10^{-6} for velocity components and temperature.

5. Code Validation

Comparison of the average Nusselt number $\overline{Nu}$ between the present study and some previous results using Darcy's model ($Da=0.01$) are shown in Table 3. As an additional check on the accuracy of the present code, normalized temperature along the mid-height of the enclosure was validated against the analytical results of Haajizadeh [8] for Rayleigh number of 100 and aspect ratio of 5 as illustrated in Fig.2.

6. Results and Discussion

The effect of varying Rayleigh number ($Ra=10^3,10^4,10^5$) on streamlines and isotherms when ($Da=0.01,\phi_1=\phi_2=\phi_3=0.02$) is shown in Fig. 3. These figures compare the streamlines (on the left) and isotherms (on the right) using ternary hybrid nanofluids as Alumina (Al_2O_3), Copper (Cu) and Titanium (TiO_2), suspended into water (H_2O). It is seen that for ternary hybrid nanofluids, a single circulation cell was observed in the clockwise directions. For higher values of Rayleigh number, the flow strength is higher than for lower values of Ra. Isotherms show almost the same distribution for these ternary hybrid nanofluids as in the case

when the cavity is filled with a simply nanofluids. In the case of $Ra = 10^3$, one can find that natural convection is not very strength inside cavity, while isotherms are nearly parallel to isothermal walls. A growth of Rayleigh number ($Ra = 10^4\ and\ 10^5$) characterizes a formation of thermal boundary layers along the both vertical isothermal walls of the cavity that start to interact with more intensive circulation. This in turn increases the heat transfer of the nanofluid as shown in Fig. 7, which indicates that the absorption of heat from the appliance is enhanced and the appliance is ensured an optimum temperature and long life. Therefore, using this combination of ternary hybrid nanofluids as coolant in motor vehicles can reduce air pollution.
Figure 4 depicts the effect of varying the volume fractions of nanoparticles ($\phi_i = 0.005, 0.01, 0.02$) on the streamlines and isotherms when ($Da = 0.01,\ Ra = 10^5$). We remark on a slowly decreasing stream field by adding nanoparticles of ternary nanofluids.

Figure 5 visually compares the streamlines between nanofluid (alumina), hybrid (alumina and copper), and ternary hybrid (alumina, copper and titania) nanofluids for various Rayleigh numbers (Da = 0.01, $\phi_1 = \phi_2 = \phi_3 = 0.02$). These confirm that the flow of ternary fluid inside the cavity is slightly slowed down by adding nanoparticles inside.

Table 3. Comparison of the average Nusselt number between the present study and some previous results using Darcy's model (Da=0.01)

Reference	$\overline{Nh}$			
	Ra*=10	Ra*=50	Ra*=10^2	Ra*=10^3
Walker and Homsy [9]	1.38	1.98	3.097	12.960
Bejan [10]	0	0	3.097	12.960
Beckermann et al. [11]	0	0	3.119	0
Gross et al. [12]	--	--	3.141	13.448
Moya et al. [13]	1.065	0	2.801	0
Manole and Lage [14]	--	--	3.118	13.637
Baytas and Pop [15]	1.079	--	3.160	14.060
Sheremet and Pop [16]	1.071	--	3.104	13.839
Lauriat and Prasad [17]	1.07	--	3.09	13.41
Trevisan and Bejan [18]	--	2.02	3.27	18.38
Nithiarasu et al. [19]	1.08	1.958	3.02	12.514
Present	**1.079**	**1.984**	**3.109**	**13.487**

$\mathrm{Ra}^* = \mathrm{Ra\ Da}$

The effect of varying Rayleigh number Ra on velocity and temperature along mid-sections of the cavity for ($Da = 0.01, \phi_1 = \phi_2 = \phi_3 = 0.02$) is shown in Fig. 6. Further, for $Ra = 10^4$, the temperature remains linearly, while for $Ra = 10^6$, the temperature varies strongly near the vertical walls, while in the core it descents slowly.

The effect of varying Rayleigh number Ra on the average Nusselt number $\overline{Nu}$ for ($Da = 0.01, \phi_1 = \phi_2 = \phi_3 = 0.02$) is shown in Fig. 7. We notice that $\overline{Nu}$ increases continuously with the increase of Ra.

Finally, Fig. 8, shows the effect of varying the volume fraction on the conductivity relative ratio k_{eff}/k_f and on the viscosity relative ratio k_{eff}/k_f for nanofluid, hybrid, and ternary hybrid nanofluid. It is noted that the ternary hybrid nanofluid has better heat transfer characteristics than that of the other because using different nanoparticles with different chemical bonds helps increase the heat transfer as each nanoparticle with its chemical bond has its own properties to take care of.

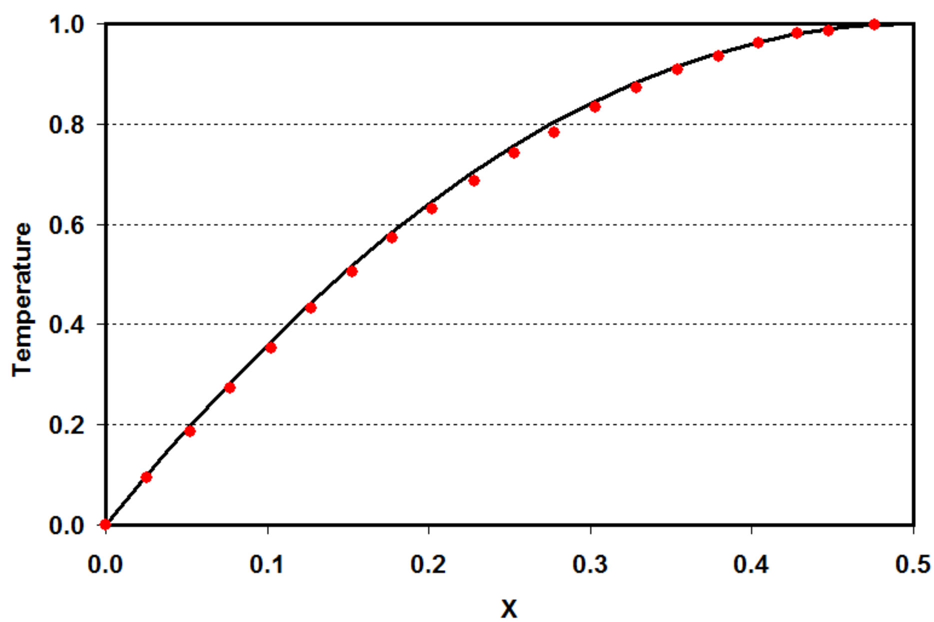

Fig. 2. Comparison of the normalized temperature along the mid-height of the enclosure using Darcy model between the present study and that of Haajizadeh et al. [8] ($\mathbf{RaPr = 100, A = 5}$).

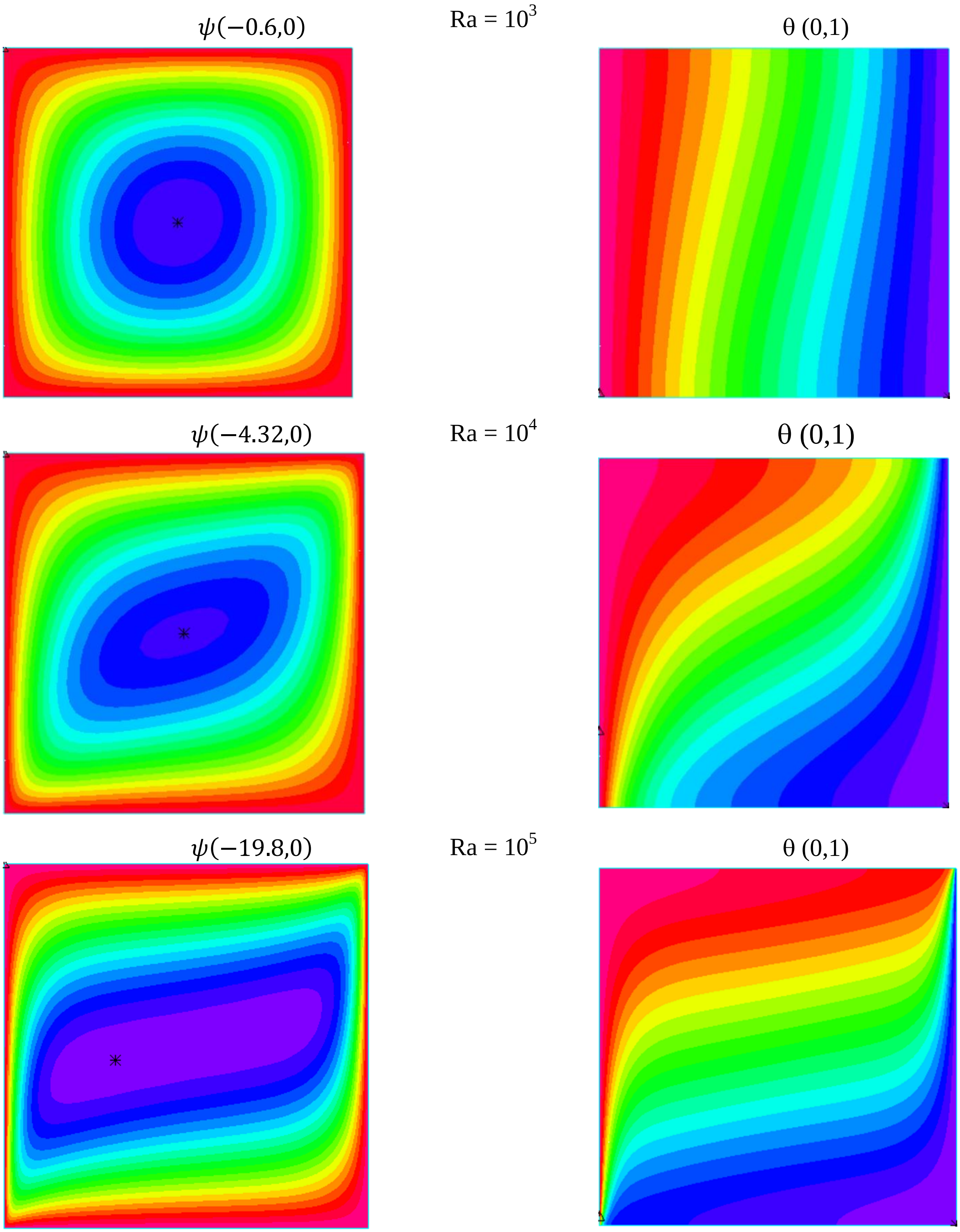

Fig. 3. Effect of varying Rayleigh number on streamlines and isotherms
($Da = 0.01, \phi_1 = \phi_2 = \phi_3 = 0.02$).

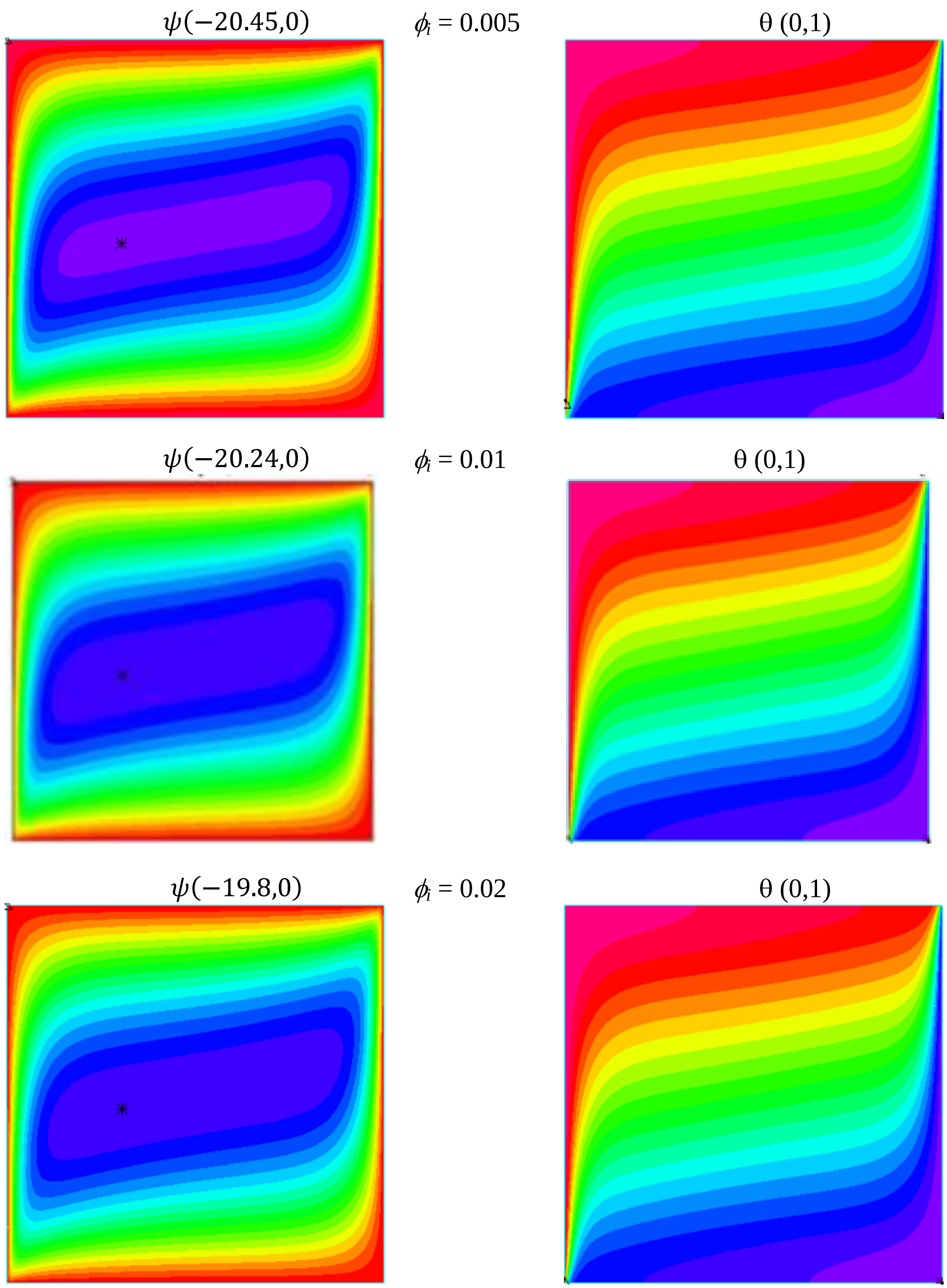

Fig. 4. Effect of varying the volume fractions of nanoparticles ($\phi_i = \phi_1 = \phi_2 = \phi_3$) on the streamlines and isotherms ($Da = 0.01,\ Ra = 10^5$)

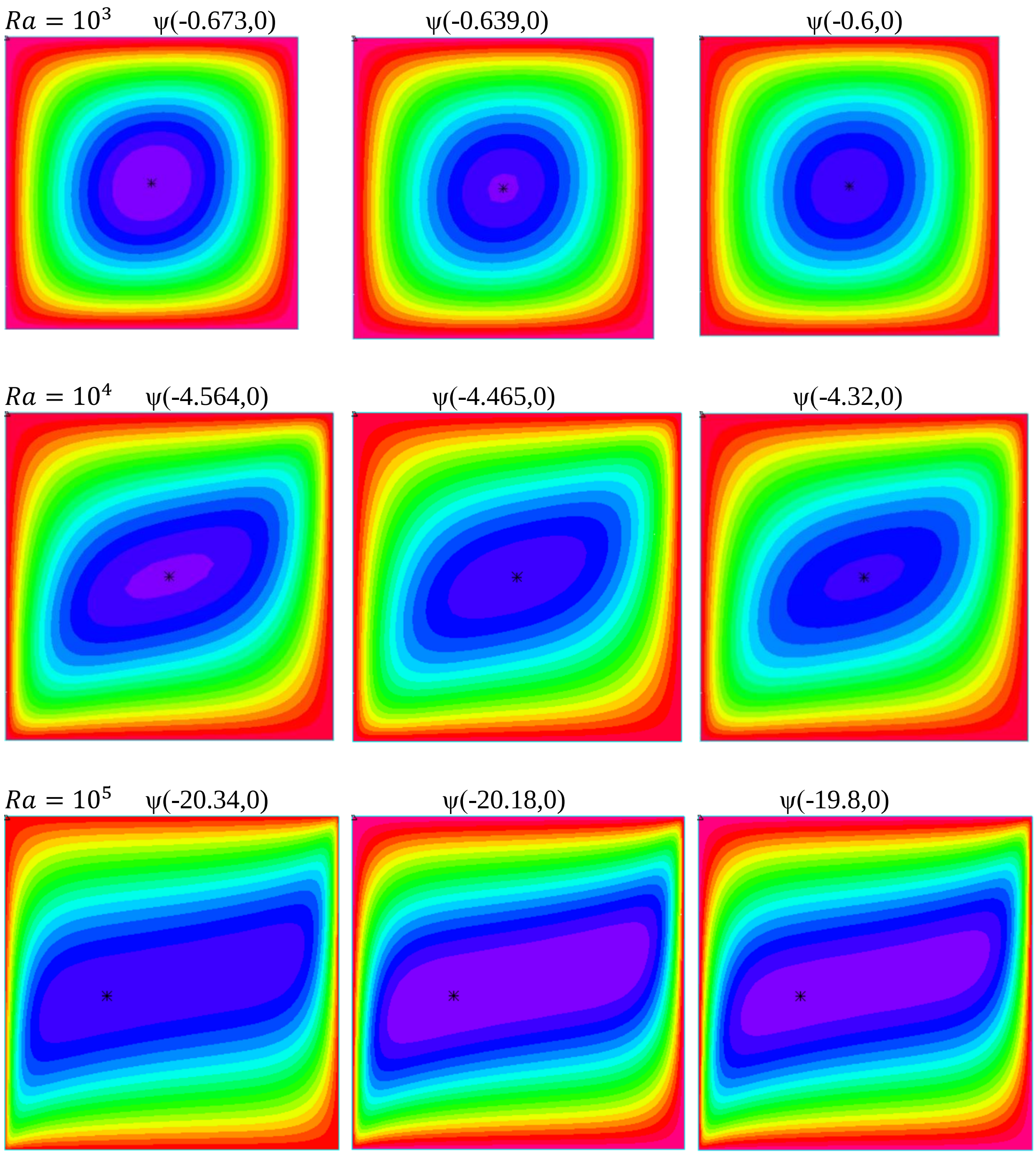

Fig. 5. Comparison of the streamlines between nanofluid, hybrid, and ternary hybrid nanofluids for various Rayleigh numbers (Da = 0.01, $\phi_1 = \phi_2 = \phi_3 = 0.02$)

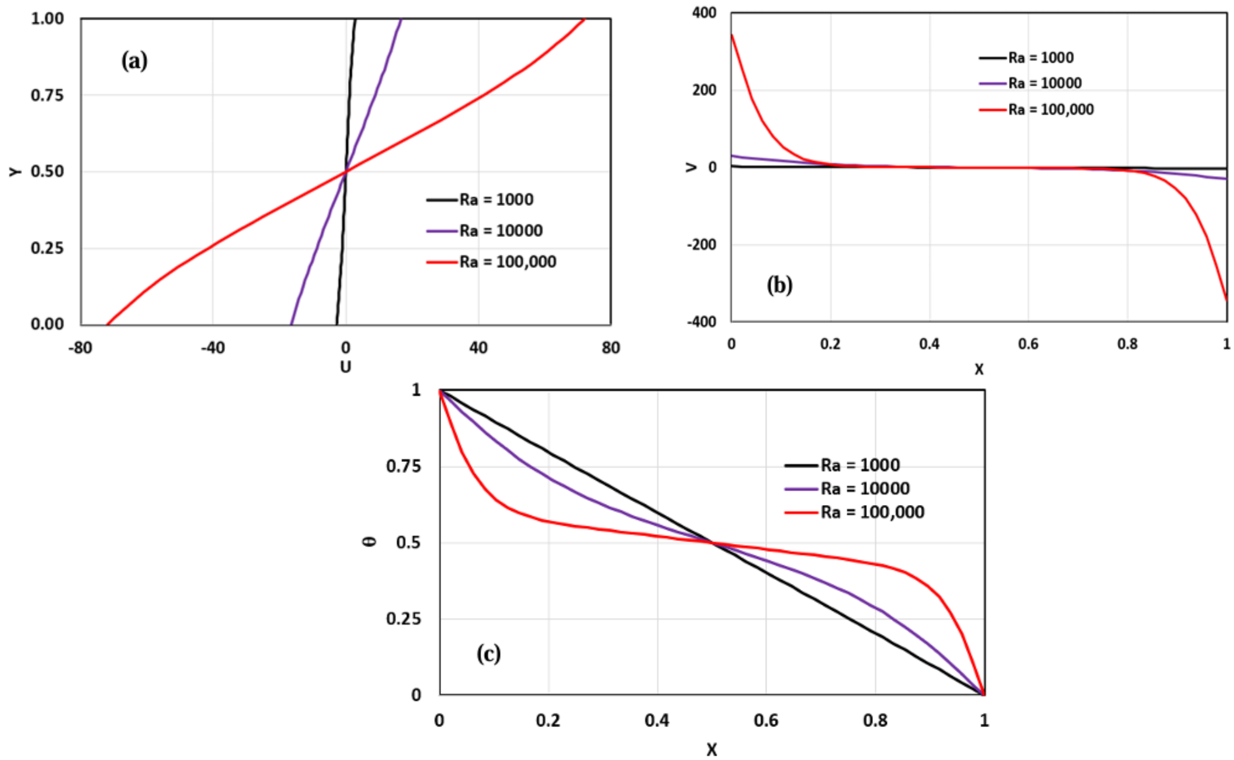

Fig. 6. Effect of varying Rayleigh number on velocity and temperature along mid-sections of the cavity $(Pr = 6.2, Da = 0.01, \phi_1 = \phi_2 = \phi_3 = 0.02)$

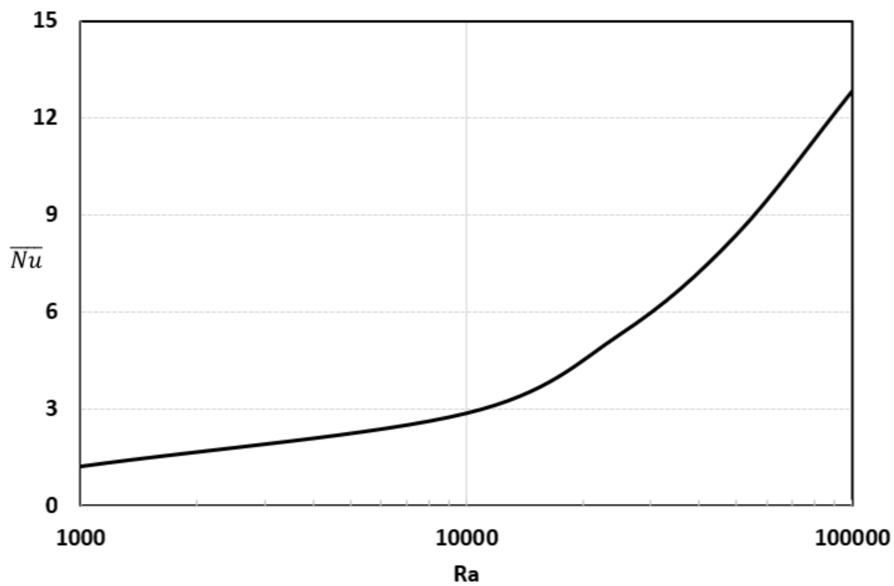

Fig. 7. Effect of varying Rayleigh number on the average Nusselt number ($Da = 0.01$, $\phi_1 = \phi_2 = \phi_3 = 0.02$)

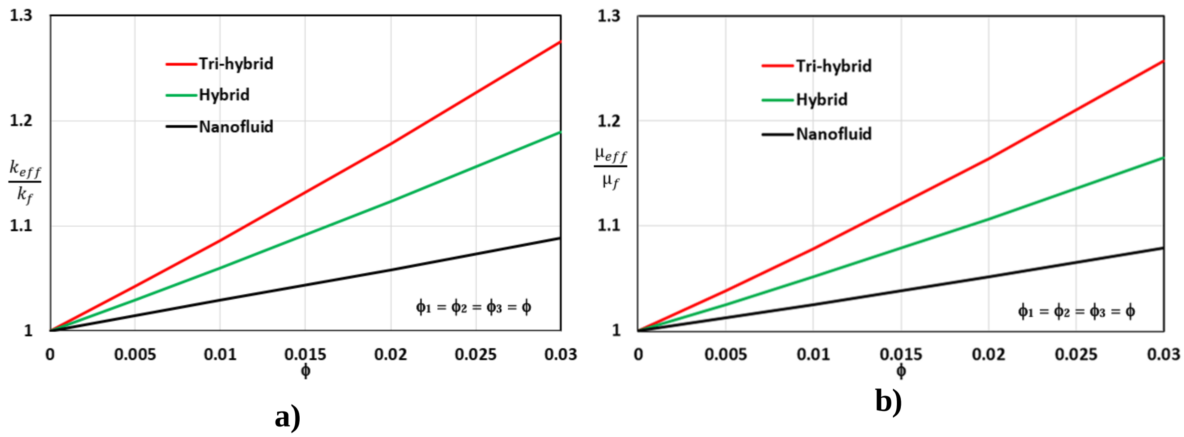

Fig. 8. Effect of varying the volume fraction on different models of (a) effective conductivity and (b) effective viscosity

7. Conclusion

The analysis of heat transfer characteristics and flow behavior for natural convection in a porous square cavity filled with a ternary hybrid nanofluid: Alumina (Al_2O_3), Copper (Cu) and Titania (TiO_2) are suspended into water (H_2O) thus forming the combination $Al_2O_3 - Cu - TiO_2 - H_2O$ is conducted. The basic dimensional partial differential equations are converted into non-dimensional differential equations. These equations are solved numerically using finite element formulation based on the Galerkin method and the results are interpreted through tables and graphs. The major outcomes of the study are:

- Ternary hybrid nanofluid has better heat transfer property than classical viscous fluid, nanofluid and hybrid nanofluid.
- The ternary nanofluid conducts more heat for higher volume fraction.
- The momentum of the flow increases for higher volume fraction.
- It is crucially yet to note that the current findings might not universally apply to all system configurations. Therefore, it is encouraged to further advance this work by exploring diverse geometries and parameter impositions, either through numerical investigations or experimental validations. Such efforts hold the promise of enriching our comprehension and refining the model, offering invaluable insights applicable to diverse practical scenarios in thermal management and engineering.

Acknowledgment

The work by Cornelia Revnic, Teodor Groșan and Ioan Pop has been supported from the Grant PN-III-P4 PCE-2021-0993, UEFISCDI, Romania.

References

[1]. Nield, D.A., *et al.*, Convection in Porous Media (5th ed.), *Springer*, *New York*, (2017).
[2]. Choi, S.U.S., Enhancing thermal conductivity of fluids with nanoparticles, *In: Proceedings of the 1995 ASME International Mechanical Engineering Congress and Exposition*, *FED 231/MD 66* (1995), pp. 99–105.
[3]. Merkin, J.H., *et al.*, Similarity Solutions for the Boundary Layer Flow and Heat Transfer of Viscous Fluids, Nanofluids, Porous Media, and Micropolar Fluids, *Elsevier, Oxford*, U.K., (2021).
[4]. Huminic, G., *et al.*, Hybrid nanofluids for heat transfer applications – A state-of-the-art review, *International Journal of Heat and Mass Transfer, 125* (2018), pp. 82-103.
[5]. Manjunatha, S., *et al*., Theoretical study of convective heat transfer in ternary nanofluid flowing past a stretching sheet, *Journal of Applied and Computational Mechanics*, *8* (2022), pp. 1279–1286.
[6]. Mahmood, Z., *et al.*, Numerical analysis of MHD tri-hybrid nanofluid over a nonlinear stretching/shrinking sheet with heat generation/absorption and slip conditions, *Alexandria Engineering Journal, 76* (2023), pp. 799-819.
[7]. Mahmood, Z., *et al.*, Numerical analysis of MHD tri-hybrid nanofluid over a nonlinear stretching/shrinking sheet with heat generation/absorption and slip conditions, *Alexandria Engineering Journal, 76* (2023), pp. 799-819.
[8]. Haajizadeh, M., *et al*., Natural convection in a vertical porous enclosure with internal heat generation, *International Journal of Heat and Mass Transfer, 27* (1984), pp. 1893-1902.
[9]. Walker, K.L., *et al*., Convection in a porous cavity, *Journal of Fluid Mechanics*, *87* (1978), pp. 338–363.
[10]. Bejan, A., On the boundary layer regime in a vertical enclosure filled with a porous medium, *Letters in Heat Mass Transfer, 6* (1979), pp. 93–102.
[11]. Beckermann, C., *et al.*, A numerical study of non-Darcian natural convection in a vertical enclosure filled with a porous medium, *Numerical Heat Transfer, 10* (1986), pp. 446–469.
[12]. Gross, R., *et al.*, The application of flux-corrected transport (FCT) to high Rayleigh number natural convection in a porous medium, *In: Proceedings of the 7th International Heat Transfer Conference*, *IS,* 1986.
[13]. Moya, S.L., *et al.*, Numerical study of natural convection in a tilted rectangular porous material, *International Journal of Heat Mass Transfer, 30* (1987), pp. 630–645.
[14]. Manole, D.M., et al., Numerical benchmark results for natural convection in a porous medium cavity, *Heat Mass Transfer in Porous Media ASME Conference, 105* (1992), pp. 44–59.
[15]. Baytas, A.C., *et al*., Free convection in oblique enclosures filled with a porous medium, *International Journal Heat Mass Transfer, 42* (1999), pp. 1047–1057.
[16]. Sheremet, M.A., *et al*., Free convection in a porous wavy cavity filled with a nanofluid using Buongiorno's mathematical nanofluid model with thermal dispersion effect, *Applied Mathematics Computation, 299* (2017), pp. 1-15.

[17]. Lauriat G., *et al*., Non-Darcian effects on natural convection in a vertical porous enclosure, *International Journal of Heat and Mass Transfer, 32* (1989), pp. 2135-2148.
[18]. Trevisan, O.V., *et al*., Mass and heat transfer by natural convection in a vertical slot filled with porous medium, *International Journal of Heat and Mass Transfer*, *29* (1986), pp. 403-415.
[19]. Nithiarasu, P., *et al.*, Natural convective heat transfer in a fluid saturated variable porosity medium, *International Journal of Heat and Mass Transfer, 40* (1997), pp. 3955- 3967.

Submitted: 27.09.2024.

Revised: 10.11.2024.

Accepted: 18.11.2024.